Numerical simulation of the acoustical properties within rocket combustion chambers

Reinhard Pongratz*, Daniel Redmann*,
*EADS Innovation Works
81663 Munich

Abstract
This document summarizes some results from a study about acoustic effect of Baffles and cavities to the acoustic field inside a combustion chamber at pure flow-acoustic conditions. Combustion process effects have not been considered. In the first part a numerical and experimental Baffle design study was done. Simulated and measured sound pressure spectra for the baffled chamber coincide very well. Spectral effects of varying baffle length and varying number of baffle blades on the acoustic field inside the combustion chamber have been simulated for a given axial flow velocity profile. Clear tendencies regarding the modal frequency shift have been identified. The result compares very well to data given in the literature. The second part reports the effect of the acoustic cavities coupled via an annular gap to the combustion chamber. The influence of gap dimensions and cavity length on the cavity acoustics was simulated. Using hot gas test results available from previous test campaigns numerical cavity design and estimation of necessary number of cavities have been done. Comparisons to data issued confirmed good comparisons.

Nomenclature

b	=	gap width
c	=	speed of sound
c_p	=	specific heat at constant pressure
d_{Hub}	=	diameter of baffle hub
f	=	frequency
k_ℓ	=	length correction factor
ℓ_{eff}	=	effective cavity length
$\Delta\ell$	=	acoustic length correction
p	=	static pressure
ℓ_B	=	baffle length
t	=	gap depth
D_{CC}	=	diameter of combustion chamber
L_{CC}	=	length of combustion chamber
M	=	molar mass
N_B	=	number of baffle blades
T	=	absolute temperature
λ	=	acoustic wave length
ρ	=	fluid density
κ	=	adiabatic exponent
$\alpha_{m,n}$	=	eigenvalue

1. Introduction

Issues, which should be answered by the preliminary numerical simulation regarding combustion chamber applications, can be summarized in the following topics: First estimation of the expected acoustic frequency spectrum and modal composition inside combustion chamber; Consideration of complex flow conditions and gas parameter gradients inside combustion chamber; Estimation of complex geometry variations on the acoustic spectral behaviour (baffles) and study and optimization of acoustic cavity tuning and design. These points are necessary for optimal design of the combustion chamber under aspect of the acoustics behaviour and consequently essential for the combustion stability. At EADS Innovation Works these numerical simulations were performed by commercial acoustic finite element method solver ACTRAN™, which was included into the internal numerical tool chain, Fig. 1. Some examples of the numerical acoustic calculations and experimental work as performed at EADS-IW are discussed in the following chapters.

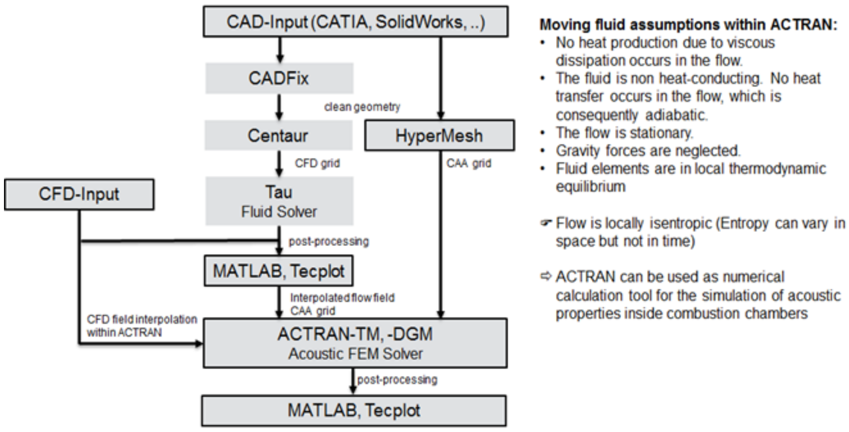

Fig. 1: Available tool chain for numerical simulations of combustion chamber acoustics

2. Numerical and experimental Baffle design study

Baffles often are cautionary for combustion chambers to prevent from thermo-acoustic combustion instabilities. When using a baffle as a passive control device, problems such as cooling and efficiency has to be accounted for. As the baffle geometry affects cooling and thrust aspects as well as its thermo-acoustic efficiency for preventing combustion instabilities the verification and optimisation of its configuration is important. For instance, the axial baffle length is recommended as approximately 20 to 30% of the chamber diameter, □[1], which might be too long regarding the above mentioned problems.

This section presents experimental and numerical results for the effects of different baffle configurations on the acoustic sound field inside a combustion chamber. Baffle height and number of baffle blades are selected as design parameters of a hub-blade baffle. Only acoustic oscillations are investigated here without any combustion effects. The experiments were pure acoustic without flow. The numerical simulations was performed with the commercial software tool ACTRAN, which is a general purpose finite element program for modelling sound propagation, transmission and absorption in an acoustic, vibro-acoustic or aero-acoustic context. With ACTRAN the convected acoustic wave equation is solved in direct frequency response mode. Therefore the Mach number in the nozzle of the combustion chamber has to be subsonic. In the model used here a maximum Mach number of 0.9 was possible and used. For this background flow a simple potential flow field was used just by the definition of an axial flow velocity on each acoustic node. A CFD solution of the internal flow field was not available. Therefore no boundary layer was defined implicating pure acoustic, loss less simulation results.

2.1 Combustion chamber geometry

The geometrical dimensions of the combustion chamber are shown in Fig. 2. The cylindrical part of the chamber has a diameter of 368 mm and is 266 mm long. The distance from the faceplate to the throat of the nozzle is 519 mm with a throat diameter of 216 mm.

The combustion chamber will use Methane and Oxygen as propellants with O/F ratio of about 3.40. The gas conditions within the chamber are summarized in Table 1.

Table 1: Gas conditions inside the combustion chamber

p [bar]	T [K]	ρ [kg/m³]	M [1/n]	c_p [kJ / kg K]	κ [-]	c [m/s]
47.0	3498.6	3.483	21.559	2.3264	1.1987	1271.8

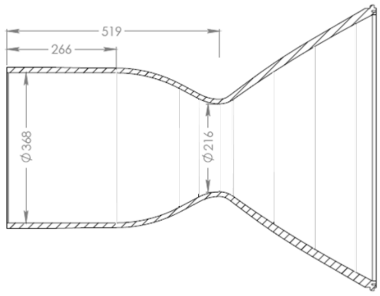

Fig. 2: Sketch and dimensions of the combustion chamber

2.2 Baffle configurations

For the numerical simulations of the effect of different baffle designs on the spectral content of the acoustic field inside the combustion chamber an n-bladed baffle with hub have been reviewed with three different baffle lengths. In addition to this length variation the number of baffle blades has also been altered. As reference the configuration as shown in Fig. 3 was defined with following dimensions:

Baffle length ℓB: 61 mm

Outer Hub Diameter: 195.4 mm

Number of radial baffle blades: 6

Wall thickness: 14.2 mm

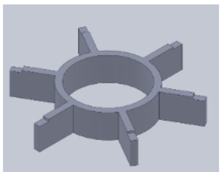

Fig. 3: Reference baffle configuration

From this reference dimensions the ratio of baffle length to chamber diameter ℓ_B/D_{CC} is 0.16 and the ratio of hub diameter to chamber diameter d_{Hub}/D_{CC} is 0.53. Following baffle design variations have been defined for the numerical study:

Baffle length ℓ_B: 45mm, 61mm, 80mm ⇒ ℓ_B/D_{CC}: 0.12, 0.16, 0.21
Number of radial baffle blades: 0, 3, 5, 6, 7

For the experimental study only the 5, 6 and 7-bladed baffle with a length of 61 mm was used. All these configurations are sketched in Fig. 4.

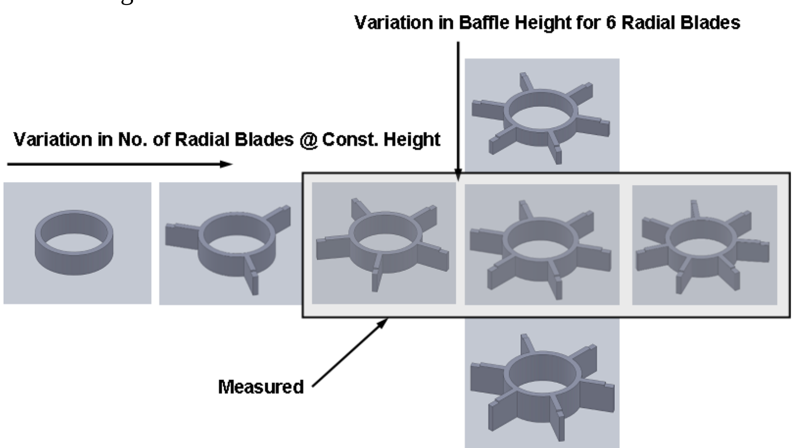

Fig. 4: Numerically studied baffle configurations

An example for a resulting baffled combustion chamber with reference baffle is given in Fig. 5. The two holes at the face plate represent the loudspeaker locations during the experiments respectively the source positions for the numerical simulations.

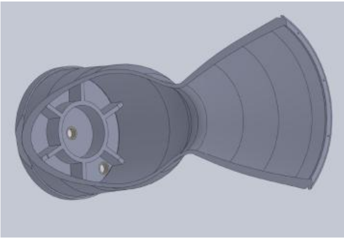

Fig. 5: Combustion chamber - reference baffle configuration

2.3 Numerical model

The design of the baffle bases on simulations using the commercial software ACTRAN. Several models and according meshes were developed for acoustic calculations. The first models represented the whole combustion chamber including divergent part of the nozzle, Fig. 6a. These models were used to validate them by measurements without flow as done at the EADS IW acoustic laboratory. Further calculations for hot gas conditions with underlined axial flow were done using the models without divergent part, Fig. 6b.

This model reduction was necessary because of the maximum possible flow Mach number of M=0.9 within ACTRAN. However all models included a 3D grid with around 0.75 million elements. For the model construction TETRA elements for fluid volume and TRI elements for surface description were used. The maximum mesh size resulted from interesting frequency range. A mesh size of 8 mm was realized. The boundary condition for all calculation was represented by hard-wall on all surfaces. In nozzle throat INFINITE ELEMENTS were used as a completion. This kind of elements was used to describe a surface without any acoustic reflection. Two sources with the same amplitude and phase were selected for acoustic excitation. These sources were placed in the faceplate, one in the middle of the chamber, on the axis of symmetry and the second on the periphery near a radial baffle blade, Fig. 6c.

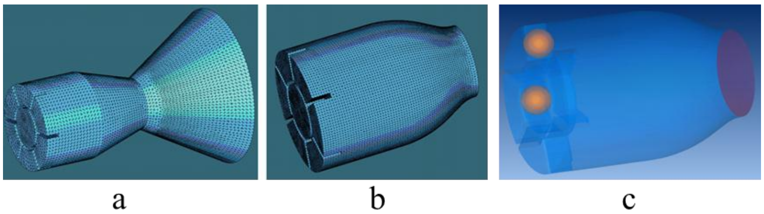

Fig. 6: Volume Meshes for the 3D-numerical model with, (a) and w/o, (b) divergent part of the nozzle and acoustic source position, (c)

2.4 Ambient conditions

In a first step simulations and experiments under pure acoustic, laboratory conditions have been done. There was no flow through the chamber and ambient gas conditions existed. Therefore the numerical model could be validated by experimental results.

2.4.1 Experimental Setup

The experimental part of the work concentrated on the effects of a hub blade baffle with 5, 6 and 7 radial blades on resonance frequencies and modal damping, (not discussed here), inside the combustion chamber. For the acoustic tests the full-scale combustion chamber was used. On the injector side a flat endplate was mounted either with the baffle included or not. Two loudspeakers are installed in the faceplate, one in the centre, the second near the chamber wall in the vicinity of a baffle blade, Fig. 7a.

A microphone was mounted on a thin rod allowing for the spatial scanning of the whole combustion chamber volume. Random noise generators were connected to the two loudspeakers mounted in the face plate supplying uncorrelated noise. The resonant frequencies were identified by spatial and temporal averaging the sound field inside the chamber. Once these frequencies are known, a sine-generator was used to activate only a particular frequency.

The shape pattern of the resulting mode could be determined by scanning the chamber in azimuthal and/or radial and axial direction for nodal lines. These lines of minimum pressure can be found first by observing the pressure amplitude and second by locating any phase shift in the chamber. The latter is done by comparing the phase between measured and a reference signal taken directly from the loudspeakers supply. A schematic lay-out of the experimental setup is illustrated in Fig. 7b.

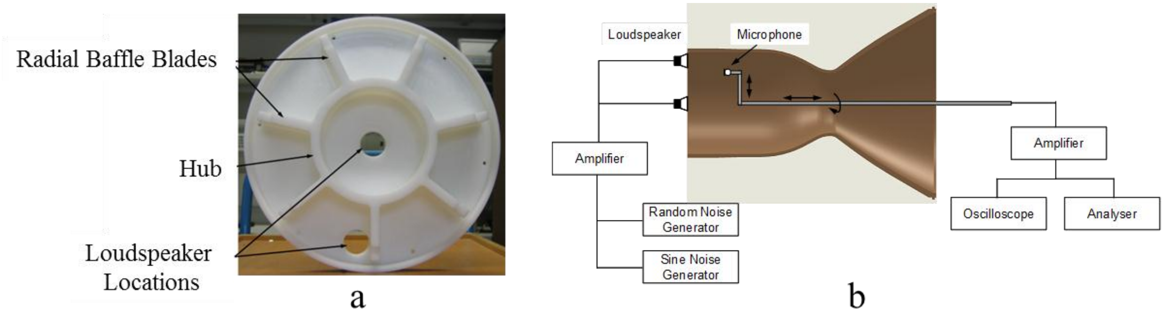

Fig. 7: End plate with a 7 radial bladed hub-blade baffle and loudspeaker openings, (a), and schematic lay-out of the experimental setup, (b)

2.4.2 Measured and Simulated Results

For the simulations at laboratory conditions without flow the whole combustion chamber including the divergent part of the nozzle has been considered. With the 6-bladed reference baffle mounted the comparison between measured and simulated sound pressure spectrum inside the combustion chamber is given in Fig. 8. Both results confirm very well. The exact deviations between the measured and simulated frequencies are given in Table 2.
The calculated modal eigen-frequencies as given within Table 2 result from the numerical ACTRAN-model (referred to as “Numeric”) and an analytic calculation scheme which solves the acoustic wave equation (referred to as “Analytic”). In case with baffle an analytical solution for transversal eigen-frequencies is given in [3] with the final formula:

$$f \approx \frac{\alpha_{m,n} c}{\pi D_{CC}} \left(1 - \frac{\ell_B}{2(L_{CC} - \ell_B)} \right)$$

As can be seen from the results as documented in Table 2 the deviations of the analytical calculations are small for lower order tangential modes. For these modes the accuracy of the estimated frequencies is satisfactory. For the T3 mode and the radial mode the results deviate more than 10% from the measured values.

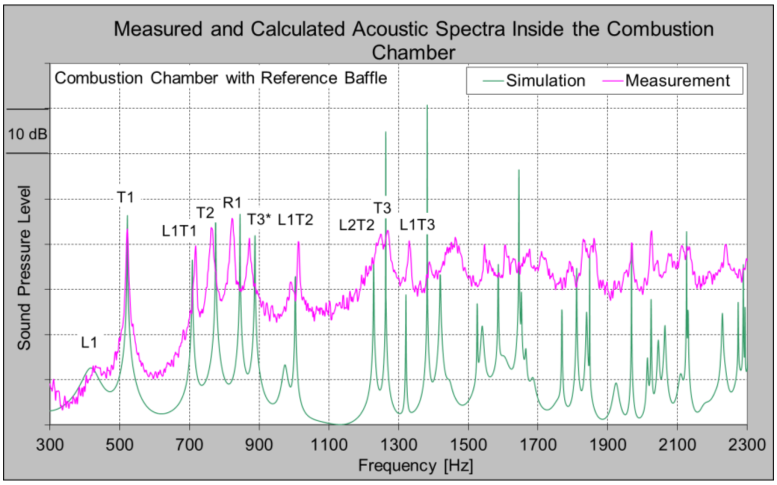

Fig. 8: Measured and simulated sound pressure spectrum inside the combustion chamber with reference baffle

Table 2: Measured and calculated frequencies of selected acoustic modes for the chamber with reference baffle

Mode	Frequency			Deviation	
	Measured	Calculation		Numeric	Analytic
		Numeric	Analytic	[%]	[%]
L1	440	424	429	-3.6	-2.5
L2	--	--	858	--	--
T1	522	522	492	0.0	-5.8
L1T1	718	708	--	-1.4	--
T2	766	775	816	1.2	6.5
L1T2	1014	1008	--	-0.6	--
R1	824	845	1024	2.6	24.3
T3*	872	888	1123	1.8	28.8
T3	1270	1263	1123	-0.55	-11.6

Due to the reference baffle the resonance frequencies for the modes L1T1, T2, R1 and T3* concentrate now between 2600 Hz and 3400 Hz. A new T3* mode appears with baffle and can propagate only within this baffle. In the un-baffled region of the combustion chamber this mode decays rapid. The spatial pressure distribution of this T3* mode is shown together with the pressure distribution of the T3 mode within Fig. 9.

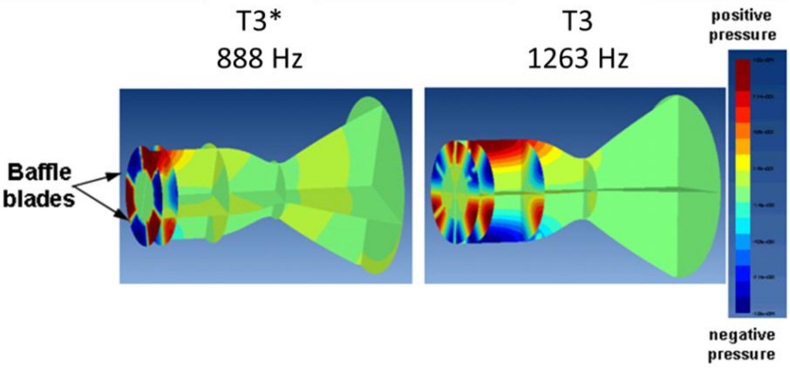

Fig. 9: Simulated spatial pressure distribution of the modes T3* and T3 within the combustion chamber with reference baffle

2.5 Hot gas conditions

As shown above was the match between simulated and measured spectra sound pressure spectra inside the combustion very good. For the laboratory case without flow the numerical model should therefore be validated. To get more realistic information about the baffle a flow field was impressed to the acoustic nodes of the numerical model. Thereby only axial velocity components are assigned to the nodes. There was no real flow field calculated. The numerical results represent therefore the solution of the convected wave equation. Complex flow effects at the baffle and therefore their effect to the acoustic damping by the baffle could therefore not be considered with this numerical model. However the effect on the frequency shift is given more realistic.
The axial velocity profile used is given in Fig. 10.

This numerical study with flow consider the effects of

- three different baffle length of a 6 hub-blade baffle
- and 0, 3, 5, 6 and 7 radial baffle blades at constant baffle length.

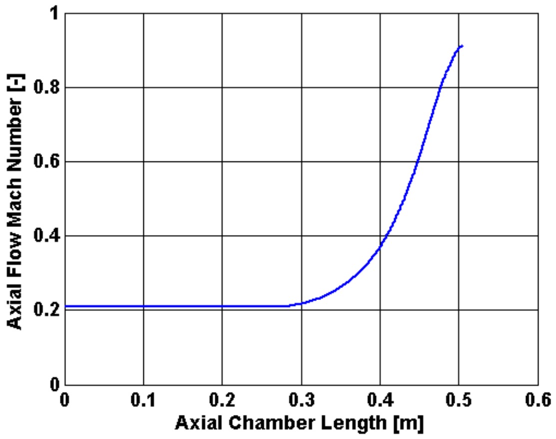

Fig. 10: Axal flow profile

2.5.1 Variation in number of baffle blades

As mentioned above, the number of radial baffle blades determines the effect of the baffle on the various tangential modes. In particular there is a difference whether the number of baffles is even or odd. According to [1] an odd number of baffles is preferable because an even number of radial baffles N_B can also be aligned with nodes of lower order $N_B/2$. Therefore numerical simulations of the modal acoustic combustion chamber frequencies with flow have been done for radial blade numbers of 0, 3, 5, 6 and 7.
The resulting sound pressure spectra inside the combustion chamber are plotted in Fig. 11. Because of clarity this diagram included only results for the baffles with 5, 6 and 7 radial blades. As was the case for the no-flow condition, again, with the 5-bladed baffle no T3* mode, now marked as $T3_B$*, can be measured. Obviously, the 5-bladed baffle offers no boundary condition for the creation of this mode

The relative frequency shift of these modes is plotted against the chamber / baffle configuration in Fig. 12. Nearly for all modes considered, the amount of frequency shift happened with the 3-bladed baffle. Only for T2 5 radial blades are necessary to shift approximately to the final value. Therefore if only the frequency shift would be considered 5 radial baffle blades with $\ell_B/L_{CC} = 0.17$ should be the enough to guarantee an effective baffle action.

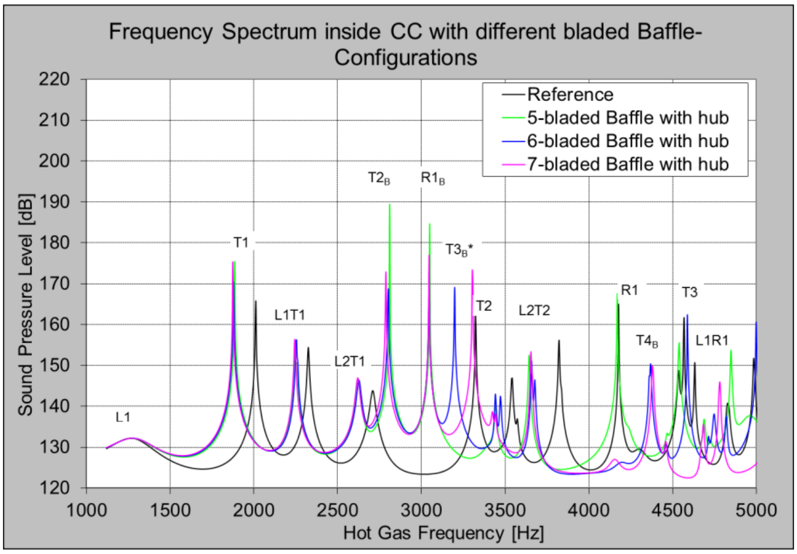

Fig. 11: Spatial averaged simulated sound pressure spectra inside CC for various baffle configurations

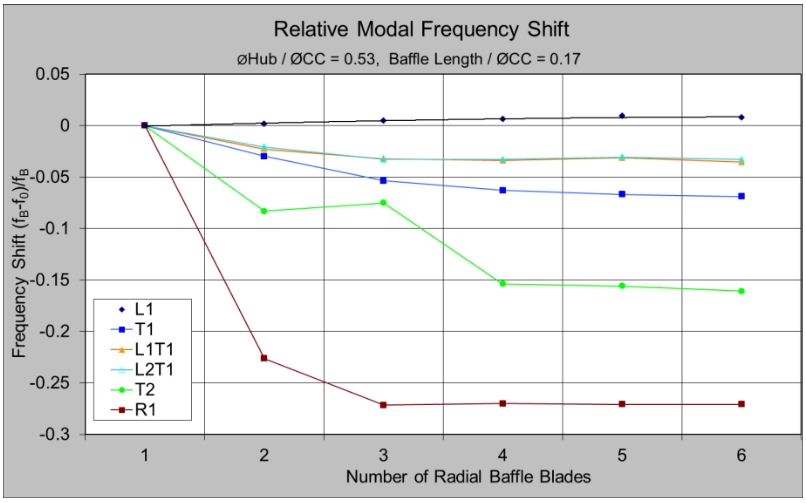

Fig. 12: Relative frequency shift of the first few modes for various baffle configurations

2.5.2 Variation in baffle length

It is well known that the baffle length is an important parameter to ensure a dynamic stable engine. "*There exist a minimum effective length below a stabilization cannot be ensured. Baffles should be made to extend continuously beyond the region of most intense combustion*.", □[1].
The 6-bladed baffle was numerically studied with three different lengths, 45mm, 61mm and 80mm resulting in length/diameter values of ℓ_B/L_{CC} = 0.12, 0.17 and 0.22. All these lengths fulfil the criterion that the baffle length should be ≥ one-fifth of the maximum baffle compartment dimension, □[1].
In the diagram of Fig. 13 the calculated frequency shift for the modes T1, T2, T3* und R1 are plotted including the measured values for the 6 bladed reference baffle. As could be expected is the frequency reduction proportional to the baffle length. Furthermore, the higher the modal order respectively the frequency the larger is the frequency reduction. The fitted trend curves are of quadratic order for the baffle length to chamber diameter ratio.
For the 1st tangential mode a reduction of the baffle length to 45 mm causes a loss in frequency reduction of about 50%. However the minimum baffle length criterion as formulated in □[1] as $\ell_B/D_{CC} \geq \pi/5N_B = 0.105$ for the 6-bladed baffle and 0.125 for the 5-bladed baffle would be fulfilled for both lengths.
The calculated frequency reduction of the T1 mode fits also well to the data published in □[2] as given in Fig. 14.

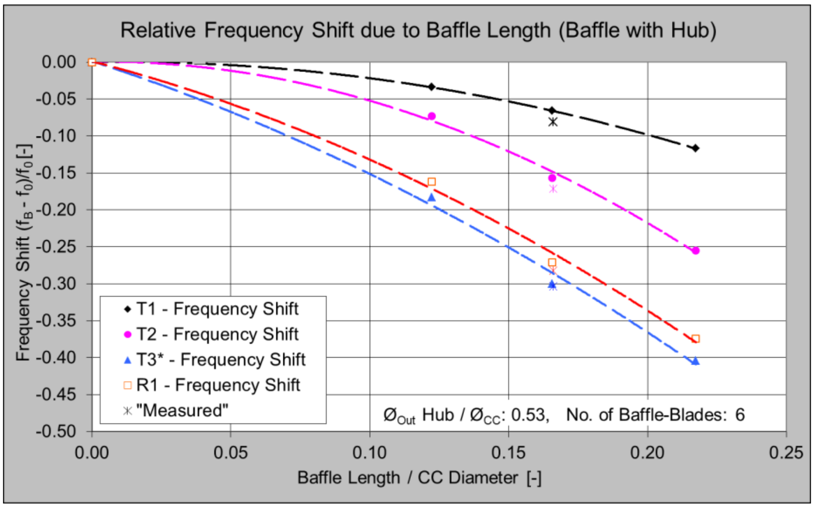

Fig. 13: Modal frequency shift due to a different length 6-bladed hub-baffle

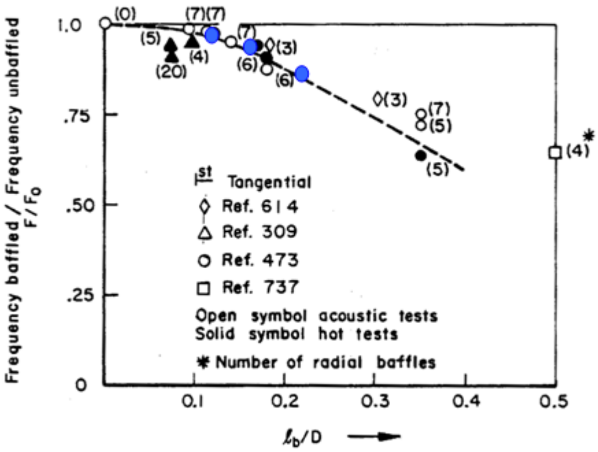

Fig. 14: Frequency depression of 1st tangential mode versus baffle length and number of baffles, [2]

2.6 Baffle design conclusion

Different hub-baffle configurations with variations in baffle length and in number of radial baffle blades were tested by pure acoustic experiments and by a numerical study. The numerical model could be successful validated by the experimental data, gathered without flow. The numerical model allowed the simulation of the various baffle geometries on the spectral characteristics of the resulting sound field inside the combustion chamber with and w/o simple non-rotational, axial flow. The experiments enabled the validation of the numerical model and made the determination of the acoustic damping by baffles with different number of radial blades possible.

It could be shown that with 5 radial baffle blades the frequency reduction of the relevant modes (T1, L1T1, L2T1, T2 and R1) reaches almost its maximum. The baffle length of 60 mm with a resulting length to diameter ratio of 0.17 exceeds the minimum baffle length as recommended for a 5-bladed baffle in [1].

3. Numerical cavity design study

Acoustic cavities are cautionary for the combustion chamber to prevent from thermo-acoustic combustion instabilities. Using cavities as passive control devices, their quantities and geometries has to be tuned to the critical thermo-acoustic modal frequencies.

This chapter presents numerical simulation results for a combustion chamber acoustics using hot gas conditions and an underlying simple axially accelerated flow field with axial velocity components only. For special modes quarter-wave resonators were tuned to these frequencies and their necessary number has been calculated. Special interest has been given to the cavity arrangement because the cavities should be coupled to the acoustic field inside the combustion chamber by an annular gap. Effects of gap depth and width on cavity design and resulting pressure transfer functions between chamber and cavities had been studied.

3.1 Combustion chamber geometry

The geometrical dimensions of the present combustion chamber are shown in Fig. 15. The cylindrical part of the chamber has a diameter of 94 mm and is 135.3 mm long. The distance from the faceplate to the throat of the nozzle is 218 mm with a throat diameter of 48.2 mm.

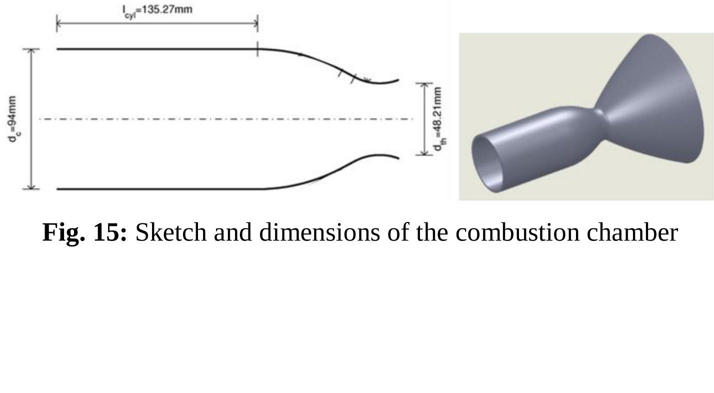

Fig. 15: Sketch and dimensions of the combustion chamber

The combustion chamber will use CH_6N_2, (MMH), and N_2O_4 as propellants with O/F ratio of about 2. The hot gas conditions within the chamber have been calculated with the CET-Code, [4], for frozen conditions and are summarized in Table 3.

Table 3: Gas conditions inside the combustion chamber

p [bar]	T [K]	ρ [kg/m³]	M [1/n]	c_p [kJ/kg K]	κ [-]	c [m/s]
14.77	3203	1.2176	21.95	2.0687	1.2242	1218.8

3.2 Cavity configurations

Within the purpose of this report the acoustic coupling of the cavities to the combustion chamber should be realised by an annular gap as sketched in Fig. 16.

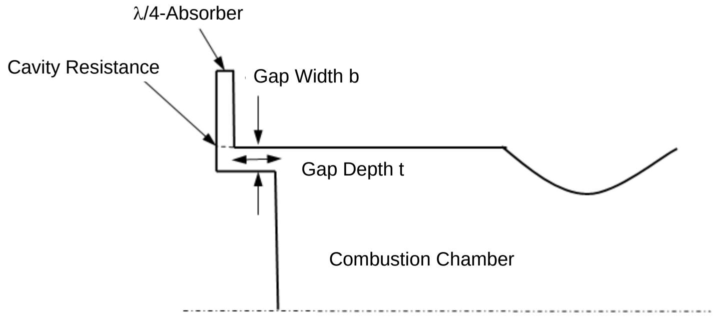

Fig. 16: Principal sketch of the cavity arrangement

Effects of gap width b and gap depth t on the cavity design parameter were studied for gap dimensions as given in Table 4. The gap depth defines the distance between faceplate and edge of the λ/4-absorber.

As reference dimensions gap width and depth values of b_{Ref} = 3.5 mm and t_{Ref} = 3.5 mm was given which are in accordance to 50 kN-values. For the absorber diameter values of 6 mm and 8 mm were defined.

Table 4: Definitions of gap width and depth to be studied

	b = 0.25*b_{Ref}	**b = 0.5*b_{Ref}**	**b = b_{Ref}**
t = 0.5*t_{Ref}			**X**
t = t_{Ref}	**X**	**X**	**X**
t = 2.0*t_{Ref}			**X**

3.3 Numerical model

For the calculation of the sound pressure spectra inside the combustion chamber a numerical model was created using the tool ACTRAN-TM. This tool is working in the frequency domain and allows the calculation of the sound field inside the combustion chamber considering complex flow effects and impedance boundary conditions. The maximum possible flow Mach number is about 0.9.
The 3D-mesh of the model was created using Hypermesh and consists of about 0.5 million elements. In order to simplify geometry variations of gab and cavities the model was build creating 2 individual meshes, one for the combustion chamber and one for the gap-cavity geometry. The number of cavities creates was 24 for the T1 mode and 12 for the T2 mode, from which a cavity spacing according to an angular displacement of 10° results. The minimum mesh size within the combustion chamber was about 7 mm whereas for the cavity mesh a minimum size 0.7 mm was chosen. The volume was built up using tetra elements and the surface by using trias elements.

In the ACTRAN-model two different acoustic finite fluids have been defined, one for the cavity-gap unit and one for the combustion chamber unit. Therefore different fluid and flow conditions could easily be simulated there. The model considers only the convergent part of the nozzle and ends at the throat using infinite elements as boundary conditions there. For the acoustic excitation two monopole sources was located at the faceplate position, one on the symmetry axis and the second at a radial distance of 40 mm. For the simulations the frequencies of the two sources were swept, starting at 4 kHz up to a maximum frequency of 18 kHz. At each step the resulting sound field was calculated. The 3D-mesh of the model is shown in Fig. 17.

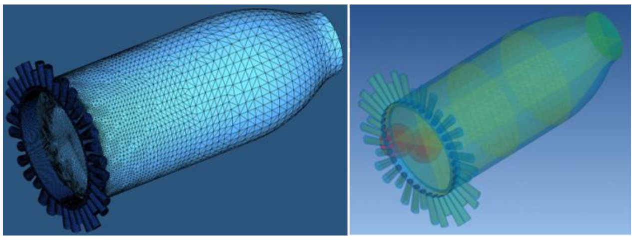

Fig. 17: 3D-mesh of the combustion chamber with cavities, gap and the two acoustic monopole sources

3.4 Combustion chamber acoustic without cavities

For the cavity design the sound pressure spectrum of the combustion chamber at reference conditions must be given. Assuming an axial flow Mach number distribution inside the combustion chamber as given in Fig. 18 the resulting sound pressure spectrum inside the combustion chamber was calculated. At the nozzle throat a Mach number of 0.9 was defined as the ACTRAN-TM model allows only subsonic flow velocities. For the cylindrical part a constant flow Mach number of 0.157 was given. By assuming this value throughout the whole combustion chamber the numerical coupling of the flow free cavity-gap partition to the chamber partition creates non-physical results. Therefore a parabolic flow velocity profile inside the cylindrical part of the combustion chamber was chosen with zero flow at the faceplate. Starting from the assumed Mach number 0.9 at the throat the velocity profile inside the converging part of the nozzle was calculated according to the nozzle geometry. For the remaining cylindrical part a parabolic velocity profile was assumed with zero flow at the faceplate. From this parabolic profile a value of 0.158 for the effective flow Mach number inside the cylindrical part of the chamber results. This effective Mach number agrees well to the pre-defined constant value of 0.157. Thus any Mach number effects on the acoustic frequencies should be considered with sufficient accuracy by the assumed velocity profile of Fig. 18.

Assuming hot gas conditions as given in Table 3 the sound pressure level spectrum as shown in Fig. 19 results. This diagram represents the spatially averaged sound pressure spectrum inside the combustion chamber as excited by the two sources. For each peak of the spectrum its modal form is written above.

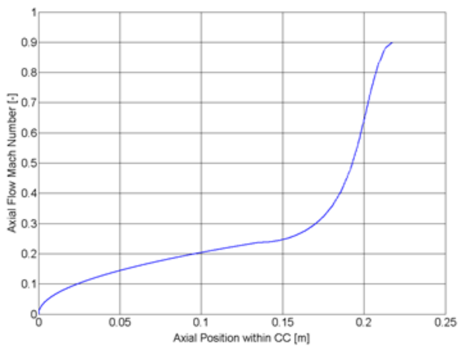

Fig. 18: Assumed axial distribution of the flow Mach number

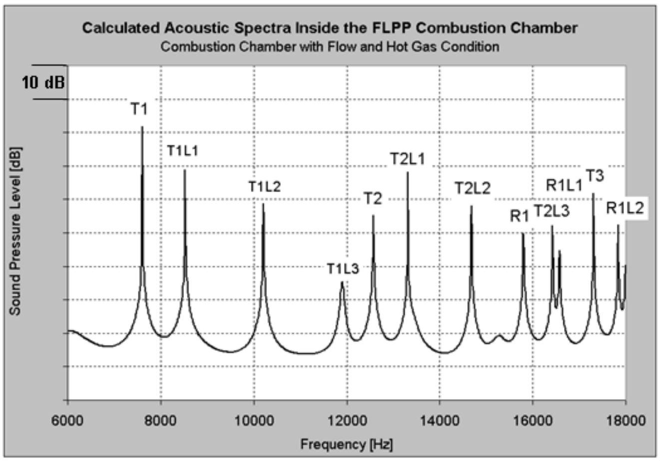

Fig. 19: Simulated sound pressure spectrum inside the combustion chamber at reference conditions

3.5 Cavity design

Within this pure acoustical study no statement on the sensitivity of the combustion process to certain acoustic modes can be done. Therefore it was decided to design the cavities for the modes T1, L1T1, L2T1 and T2.

3.5.1 Calculation of the acoustic cavity length

One critical aspect for a reliable cavity design is the knowledge of the gas properties inside the cavities, especially the temperature gradient. For the actual cavity arrangement with annular gap measurement data from formerly done tests with a 50 kN chamber are available. This combustion chamber was equipped with 2 rows of cavities at which one cavity row was coupled via an annular gap to the chamber. The cavity arrangement for this 50 kN chamber is given in Fig. 20. The cavity diameter has been 8 mm. Gap height was 3.5 mm, its length as measured from faceplate to the edge of the borehole was also 3.5 mm. Therefore an overall gap depth of 8 mm + 3.5 mm = 11.5 mm resulted.

During hot firing tests temperature and dynamic pressure inside different length cavities have been measured. Together with dynamic pressure data at the faceplate the acoustic resonance frequencies of different length cavities could be calculated.

Knowing the temperature gradient inside a cavity then the acoustic effective cavity length ℓ_{eff} could be calculated. However, no sufficient temperature data inside the cavity boreholes was available. From the hot- and cold-gas measurement data of the 50 kN campaign a mean length correction factor of about $k_\ell = 0.2$ could be extracted for the cavities behind the annular gap. Using this factor, effective cavity lengths result, which are 20% longer as the borehole lengths. Now, an effective speed of sound and effective temperature inside the cavities can be calculated. Fig. 21 shows a typical result for the effective speed of sound as re-calculated from the 50 kN test results. In this diagram a curve fit for the effective speed of sound data was done assuming a minimum effective speed of sound as indicated by the 50 kN data and a maximum effective speed of sound as given inside the combustion chamber. Under these assumptions the effective cavity length calculates to 22.8 mm for the T1 mode, with an effective speed of sound of 695 m/s. The effective temperature for this cavity calculates to 775 K.

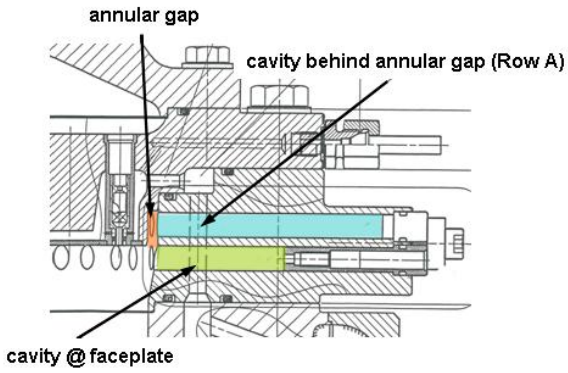

Fig. 20: 2-row cavity arrangement at the 50 kN combustion chamber

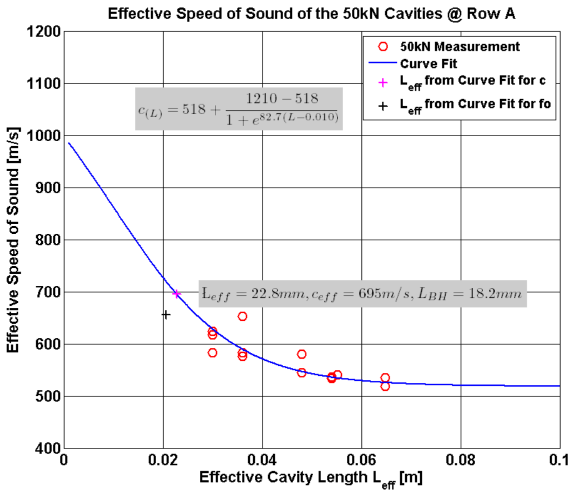

Fig. 21: From 50 kN measurement data re-calculated effective speed of sound for the T1 mode of the actual combustion chamber

For the case with reference gap dimensions, b_{Ref} = 3.5 mm and t_{Ref} = 3.5 mm, the resulting data for acoustic length, effective speed of sound and borehole length are given in Table 5 for the cavities tuned to modes, T1, L1T1, L2T1 and T2 by assuming the mentioned length correction factor of $k_\ell = 0.2$. The exact length fine tuning has in any case to be done during hot firing tests on a representing hardware.

Table 5: Acoustic length, effective speed of sound length correction of cavities tuned to the given modes

Mode	$\ell_{acoustic}$ [mm]	c_{eff} [m/s]	ℓ_{BH} [mm]
T1	22.8	695	18.2
L1T1	21.0	716	16.8
L2T1	18.3	748	14.7
T2	15.6	784	12.5

3.5.2 Effect of gap dimension

In order to gain more information about the influence of the gap dimensions on cavity resonance frequencies and impedances pressure transfer functions between combustion chamber and cavities have been calculated for gap dimensions defined in Table 4. Several microphones have been placed inside two cavities of the numerical model described above. The cavities chosen have been tuned to T1 and T2. A common speed of sound with a value of 775 m/s was assumed for all cavities. The microphone numbering and arrangement for the two cavities is sketched in Fig. 22.

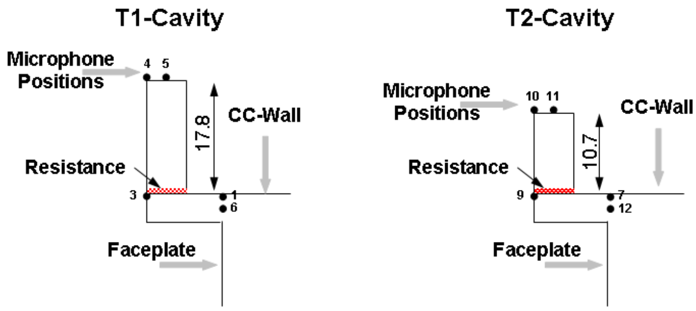

Fig. 22: Microphone arrangement at the cavities for estimation of pressure transfer functions

For the T1-cavities the length of the cylindrical borehole was 17.8 mm and for the T2-cavities 10.7 mm. The cavity diameter was 6 mm.

For the realisation of a cavity resistance in the numerical model two calculation domains have been created, one for the fluid inside the cylindrical boreholes of the cavities and one for the rest of the volume consisting of combustion chamber and annular gap. The two domains were coupled via transfer matrices which defines the acoustic transfer admittances from the gap to the cavities. This resistance values have also been extracted from the 50 kN measurements. Introducing this resistance values into the matrix for the transfer admittances between the two numerical calculation domains the resulting pressure transfer functions for the cavities can be calculated. A typical result is presented in Fig. 23 where the complex pressure transfer functions between microphones 5/6, 4/1, 4/3 and 3/1 for a cavity tuned to T1 are plotted. The red curves represent the imaginary parts and the blue ones the real parts.

First it can be recognized that the pressure ratio between microphones 5 and 6 equals the ratio between microphones 4 and 1, which could be expected as for both combinations the transfer functions was calculated over the identical length. It makes no differences whether the microphones are located on the symmetry axis of the cavity or not. Resonance frequency f_0 and bandwidth Δf can directly be extracted from the curves. For this cavity a resonance frequency of 7817 Hz can be extracted, for which an effective acoustic cavity length of 24.8 mm results. This length can approximately be found in the cavity geometry by summing up the borehole length, half the diameter of the borehole, half the gap width and gap depth, $\ell_{bh} + d/2 + b/2 + t = 26$ mm, which follows the symmetric axis of the 2D-sketch in Fig. 22. In addition, both diagrams show also some effect of the T2-cavity.

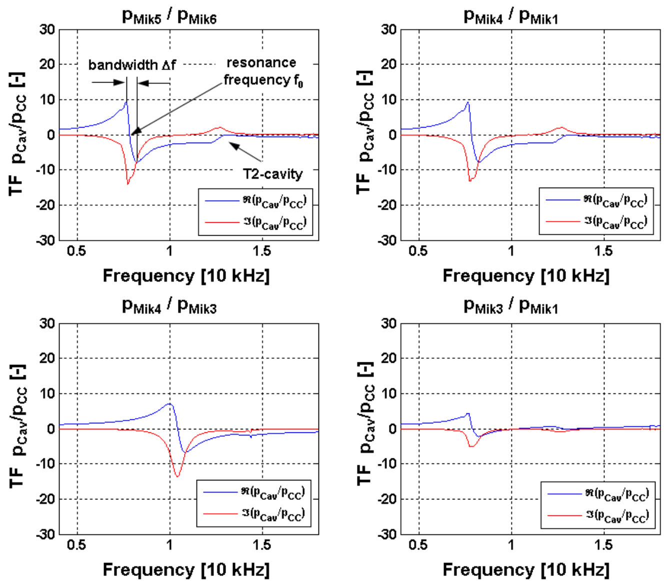

Fig. 23: Simulated pressure transfer functions between different microphones of the cavity tuned to T1 for reference annular gap dimensions (b = t = 3.5 mm)

The pressure ratio 4/3 considers only the cylindrical borehole. Accordingly, the resonance frequency is higher and, in addition the pressure ratio looks smoother compared to the ratio if the annular gap is considered.

The forth diagram gives the ratio over the gap depth. At this position the resonance frequency equals that as resulting from the microphone positions 5 and 6 but the pressure ratio at resonance is only a fraction of the ratio as measured over the whole cavity length.

In order to get an idea how the gap dimension acts on the resulting resonance frequencies of the cavity the resulting frequencies are plotted in **Fehler! Verweisquelle konnte nicht gefunden werden.** for the cavities tuned to T1.
This diagram shows contrary effects for the two gap dimensions varied on the cavity resonance frequencies. The cavity resonance frequencies increase if the gap length t is reduced for constant gap width or if the gap width is enlarged while keeping t constant. If the gap length is reduced at constant b, the acoustic length of the cavity diminishes and hence its resonance frequency rises. On the other hand, if the width of the gap is enlarged the remaining borehole behaves more and more independent, the gap becomes part of the surrounding fluid and its effect on the cavity diminishes. Similar results are obtained for the cavity tuned to T2.

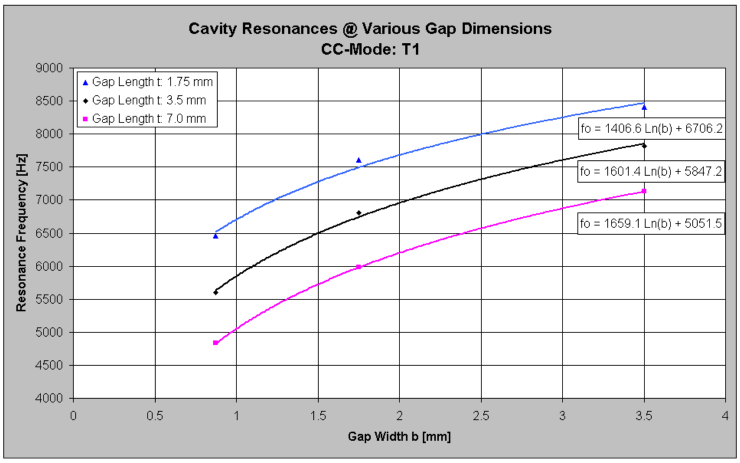

Fig. 24: Resonance frequencies of the T1-cavities at various gap width and gap length

The combination of borehole and gap can acoustically result in a Helmholtz resonator with the gap acting as neck and the borehole representing the volume. This can be expected especially for narrow and short gaps. In case of deep gaps with medium widths the resulting dynamic behaviour of the cavity build up by borehole and gap can result from the coupling of two independent $\lambda/4$-cavities, borehole and gap with different cross sectional areas. The resonance frequencies of this coupled system would not only depend on the length of the two individual resonators (borehole and gap) but also on the relation of their cross sectional areas.
For example, the resonance frequency for the combination of the 17.8 mm long borehole and the gap with t = 1.75 mm and b = 0.875 mm is 6460 Hz at simulation conditions. For this frequency an acoustic effective length of 30 mm can be calculated which is much longer than the sum of borehole length and gap depth, 19.55 mm. This situation becomes more obvious if one compares the length correction related to the wave length at resonance with the ratio between gap width and square root of gap length time's borehole length, as done in Fig. 25. This diagram confirms a clear relation between borehole / gap dimensions and the resulting relative acoustic length correction for both cavity tunings, T1 and T2. As this relation is derived using the well-known formula for the calculation of the resonance frequency of a Helmholtz resonator the combination of a gap with a borehole tends to be represented by such an acoustic resonator type.
Besides its influence on the resulting cavity resonance frequencies the gap affects also the qualities of the pressure transfer function. The pressure transfer function shows best results for the shortest gap length. If this length is enlarged the transfer function differs remarkably from that of an SDOF absorber. It is worst for a long and narrow gap. Therefore, the recommendation is to design the gap short (t = 1.75 mm).
The width influences the magnitude of the pressure transfer function. The smaller the width the lower is the magnitude of the pressure transfer function indicating for an increasing acoustic resistance. If the length of the borehole is critical the width should be made small because a reduced resonance frequency result and therefore a shorter borehole design become possible.

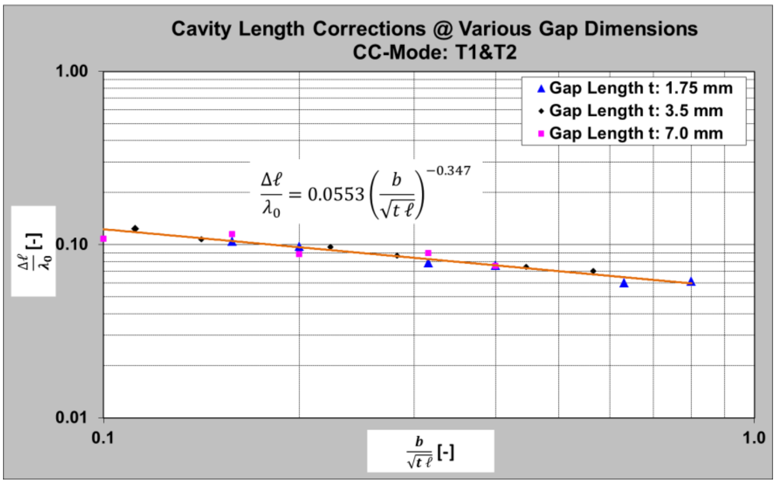

Fig. 25: Relation between length correction and gap & borehole dimension for the T1 and T2 cavities

3.5.3 Estimation of necessary number of cavities

The necessary number of cavities was estimated in two different ways. First, 100% absorption should be realized inside the combustion chamber. To get this absorption the sum of the impedances off all cavities should be one at the frequency of the specific mode. Knowing the impedances of the individual cavities the necessary number of cavities to fulfil this postulation can be estimated. The resistance can be calculated from the 50 kN data as mentioned above.
The second approach tries to account for the modal intensity distribution inside the combustion chamber and to calculate the acoustic energy of the mode. Knowing the cavity resistance the energy absorbed per cycle at resonance can be calculated and the necessary number of cavities can be estimated. Assuming for the acoustic pressure amplitude a value of 5% of the static pressure inside the combustion chamber and using the cavity resistance values as given from the 50 kN data absorption and normalized impedance result as given in the diagrams of Fig. 26. Within these diagrams the numbers of cavities are given for both calculation schemes. With both formulations similar results have been obtained.

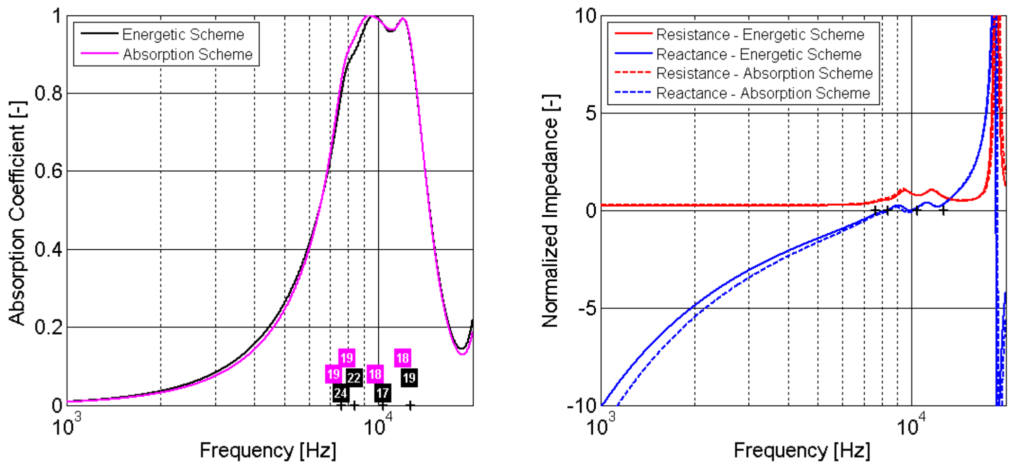

Fig. 26: Comparison of absorption coefficient and normalized impedance for the energetic and impedance based calculation scheme for a T1, L1T1, L2T1, T2 - cavity tuning

Knowing the number of cavities, using a cavity diameter of 8 mm and the chamber diameter the fractional open area can be calculated. These results are plotted in the diagram for the absorber effectiveness as given in Fig. 27. This diagram confirms that for both calculation schemes, the resulting fractional open areas for all four modes are well above the data as recommended by the NASA-SP 8113, [5] Therefore, a good stabilization effect of the cavity tuning suggested could be expected.

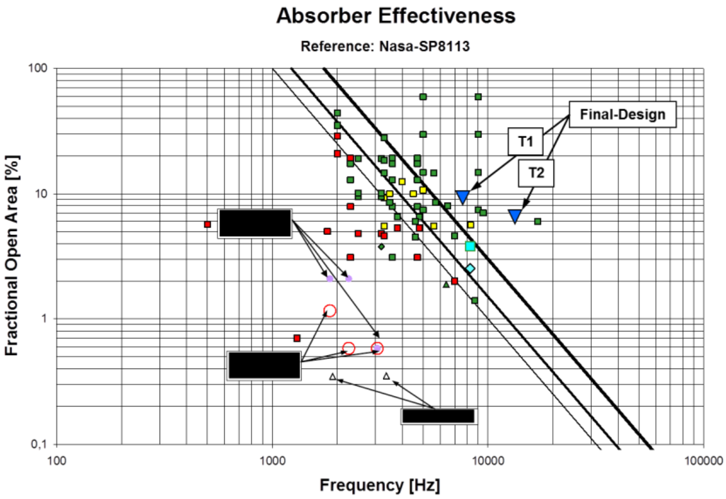

Fig. 27: Absorber effectiveness for the calculated number of cavities

The effect of the cavities on the sound field inside the combustion chamber was simulated with the ACTRAN model described in section 3.3. As mentioned there, for all cavities a constant speed of sound of 775 m/s was assumed. 24 cavities were tuned to T1 and 12 cavities were tuned to T2. The normalized resistance of a single cavity were set to 0.06 for both types. The resulting, spatially averaged sound pressure spectrum inside the combustion chamber is plotted in Fig. 28 for both cases without damping and damped. Due to damping and detuning effect of the cavities the pressure amplitudes are reduced severely.

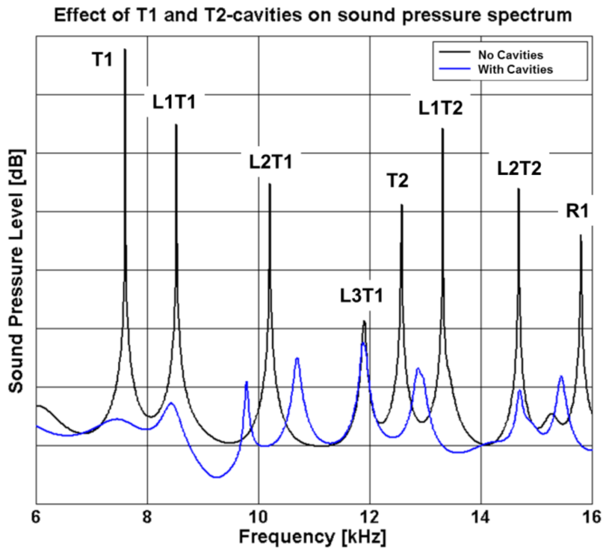

Fig. 28: Comparison of the spatially averaged sound pressure spectrum inside the CC with and without cavities for a gap geometry according to b= 3.5 mm and t = 3.5 mm

4 Conclusion

The aim of this paper was the study of combustion stabilisation devices as Baffles and cavities and their interaction with the combustion chamber acoustics at pure acoustic conditions, without regarding any combustion processes. It could be shown that using adequate numerical models together with necessary experimental data a preliminary design on baffle and cavity geometry is possible. For both stabilisation devices the results compare very well to data issued within the literature. Preliminary design of acoustic damping devices can therefore be done without exact knowledge of specific combustion effects with good reliability.

References

[1] NASA, "Liquid Rocket Engine Combustion Stabilization Devices", NASA, SP-8113, 1974, p 17
[2] NASA, "Liquid Propellant Rocket Combustion Instability », NASA, SP-194, 1972
[3] M.S. Natanzon, "Combustion Instability, Progress in Astronautics and Aeronautics", Volume 222, p. 123
[4] S. Gordon, B.J. McBride, "Computer Program for Calculation of Complex Chemical Equilibrium Compositions and Applications", NASA RP 1311, October 1994
[5] NASA SP 8113, "Liquid Rocket Engine Combustion Stabilization Devices", November 1974